The Way to Spray: Modeling Nasal Spray Deposition

BEE 453: Computer-Aided Engineering

April 30, 2009

Amrita Mahtani

Guilly Mendoza

Weilin Yang

Robin Zhou

Table of Contents

1. Executive Summary

Intranasal drug delivery is an alternative method in addition to traditional oral and intravenous doses. Nasal drug delivery has proven to be a very effective technique for nicotine cessation (Hjalmarson *et al.*, 1994), the influenza vaccine (Jackson *et al.* 1999), and drugs that need to be take continuously, such as insulin (Dondeti *et al.*, 1995).

Studies have found that for effective fast-acting body response, the drug needs to be deposited in the highly vascularized mucosal tissue lining the bony turbinates in the nasal cavity. Commercial nasal sprays are continuously optimizing parameters to develop the most effective deposition patterns.

In this project, drug deposition is modeled using a simplified 2D depiction of the nasal passageway with uniformly-shaped, spherical spray particles. This problem is implemented in COMSOL by using 2D Navier Stokes fluid flow equations to model the airflow through the nose, and the Particle Tracing module to model the spray trajectory and deposition.

The model output was validated by determining the percentages of particles in each region of the nasal passage – anterior, turbinate, posterior, and outlet – and comparing with published experimental data by Cheng *et al* (2001).

A sensitivity analysis was done on the following parameters: particle density, particle size, nozzle spray angle, and nozzle penetration depth. It was found that this model was sensitive to only penetration depth. As penetration depth through the nostril increased, there was a decrease in the particle deposition in the anterior region of the nasal cavity and an increase in the percentage of particles that exited through the outlet. Deposition in the middle and posterior regions was not affected by variation in penetration depth. Our sensitivity analysis demonstrated that variations in spray angle, particle size, and density of the nasal spray fluid do not significantly affect deposition pattern. Therefore, when designing nasal sprays, as long as these parameters remain within the specified ranges, consistent deposition patterns will be achieved. This result also allows for further research on creating sprays that are more concentrated and have encapsulated drugs.

Keywords: *intranasal spray, particle deposition, drug delivery*

2. Introduction

The nasal cavity contains three turbinates, which are long shelves of spongy bone that divide the nasal passage into three airways. These airways are lined by mucosa, a highly vascularized tissue with openings to the paranasal sinuses. It has been hypothesized that drug deposition onto the mucosa lining of these turbinates can potentially treat health problems such as lung diseases, cancers, diabetes, and sinus infections (Inthavong *et al.* 2008). This has motivated many studies about nasal drug delivery systems (Cheng *et al*, 2001; Kimbell *et al*, 2007; Pringels *et al*, 2006; Sharma *et al*, 2009).

Drug delivery through the use of nasal sprays is a unique alternative to the more traditional oral or intravenous administration of drugs. Nasal sprays can produce a faster response to the blood stream or area of interest than oral applied drugs, and does not degrade the drug as it travels through the digestive system (Inthavong *et al.* 2008).

The liquid mixture of nasal sprays is converted to a fine spray composed of micron-sized particles. These particles enter the nostril, travel through the nasal cavity, and deposit within the passage way. It has been found that the majority of drug material is deposited within the anterior portion of the nose; however, this is disadvantageous as this area contains filters and narrow passageways to restrict large drug particles from being absorbed within the more vascularized mucosal walls. Deposition in the mucosal walls of the turbinates would allow the drug to diffuse into the blood stream and provide relief for a patient (Inthavong *et al.* 2008).

Inthavong *et al.* (2008) performed a study to determine the parameters important in designing a nasal drug delivery device. In order to do this, two visualization systems were used: (i) a particle/droplet image analyzer (PDIA), and (ii) particle image velocimetry (PIV). The PDIA provides detailed imaging of the spray and formation of droplets and the PIV gives an approximate velocity field. The researchers used FLUENT and employed the Lagrangian particle movement equations to trace the dispersion and trajectory of particles. They determined that the parameters particle size, diameter of spray cone at a break-up length, and spray cone angle had significant effects on deposition.

Since the effects of spray cone angle and diameter of spray cone at break-up length have already been determined, we examined other parameters. We used the same equations (Inthavong *et al.*

2008) to model movement of particles in our simulation and have examined the effects of particle size and density, as well as the angle and penetration depth of spray nozzle insertion.

2.1 Design Objectives

We will determine nasal spray particle deposition within a simplified nasal cavity geometry by modeling airflow through the nasal passage along with the movement of particles. Our objective is to examine the effects of particle size, particle density, spray angle, and penetration depth of spray nozzle on the pattern of spray deposition. These terms are defined below in Problem Formulation. Ultimately, our goal is to determine what combination of spray size, density, angle, and penetration depth will lead to an optimal spray deposition within the turbinate region. Our findings can then be used to inform future designs of nasal spray delivery systems.

3. Problem Formulation

3.1 Terms Defined

Particle Size refers to the diameter chosen for the particle sphere. We have modeled drug particles as uniform spheres as this corresponds to the shape of the spray exiting the nozzle. From literature research, it was determined that the range of particle size is 10-70µm (Inthavong *et al.*, 2007; Kimbell *et al.*, 2007). We have chosen our baseline particle size to be 50µm.

Particle Density refers to the apparent density of each nasal spray droplet. This parameter would take into account the weighted averages of all spray particle components. For this study, we have chosen a baseline value of 1000 kg/m^3, the density of water (Inthavong *et al.* 2008).

Spray Angle refers to the particle angle that exits the nozzle upon applying pressure to the container. This parameter was varied when changing the initial velocity of the particle in both the x and y direction. The baseline condition was 45˚.

Penetration Depth refers to the initial depth at which the spray nozzle is inserted into the nose. As there are restrictions for this depth, we chose the baseline condition at the inlet of the nose at a depth corresponding to zero.

3.2 Schematic

We are using COMSOL to model the nasal cavity in two dimensions. A complete schematic of our model with boundary conditions and property values is shown below (Figure 1). The geometry of the nasal cavity was simplified to include only the lower turbinate, neglecting flow above the middle turbinate, based on the assumption that drug flow occurs predominantly around the lower turbinate. Figure 2 shows a more anatomical, 3D representation of the nasal passageway.

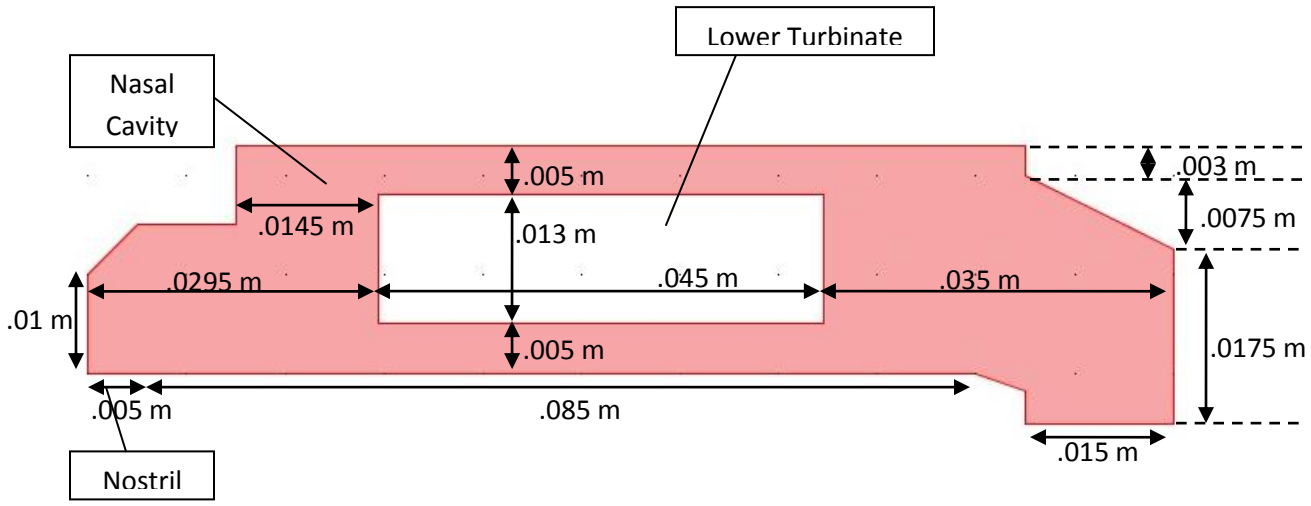

Figure 1. Schematic used in COMSOL modeling showcasing all dimensions.

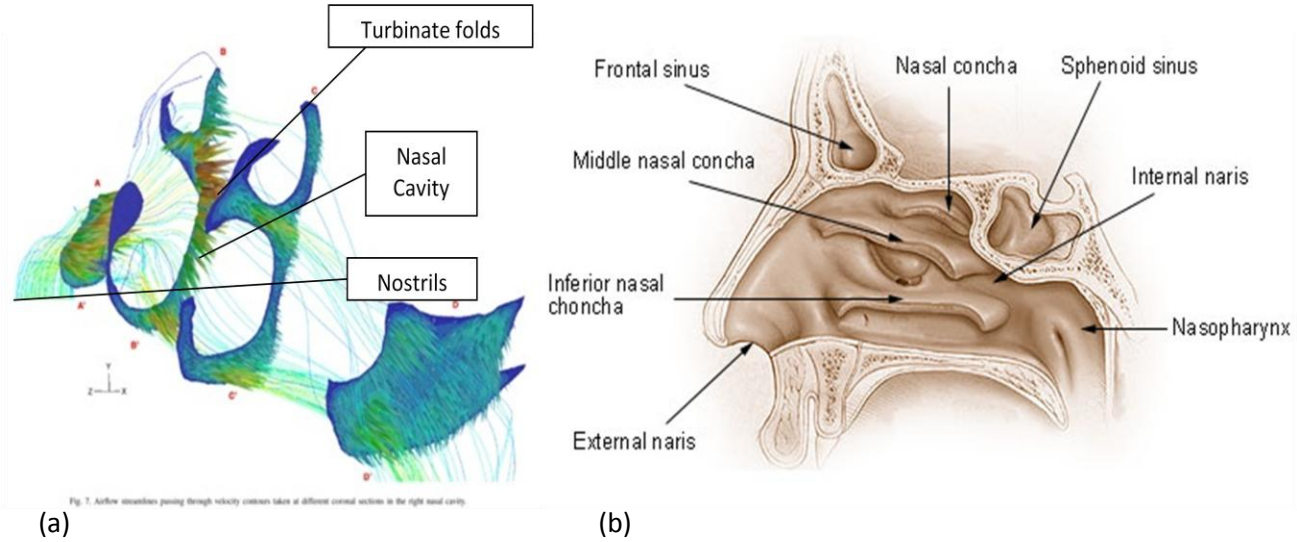

Figure 2. Actual 3 dimensional geometry of nasal cavities. (a) Taken from Inthavong *et al.* 2008; (b) Taken from Wikipedia under the GNU Free Documentation License. Note, nasal concha is another term for the nasal turbinate folds.

3.3 Mesh

We used an unstructured mesh, with an "extra fine" predefined mesh size, shown in Figure 3. This mesh contained 4624 triangular elements.

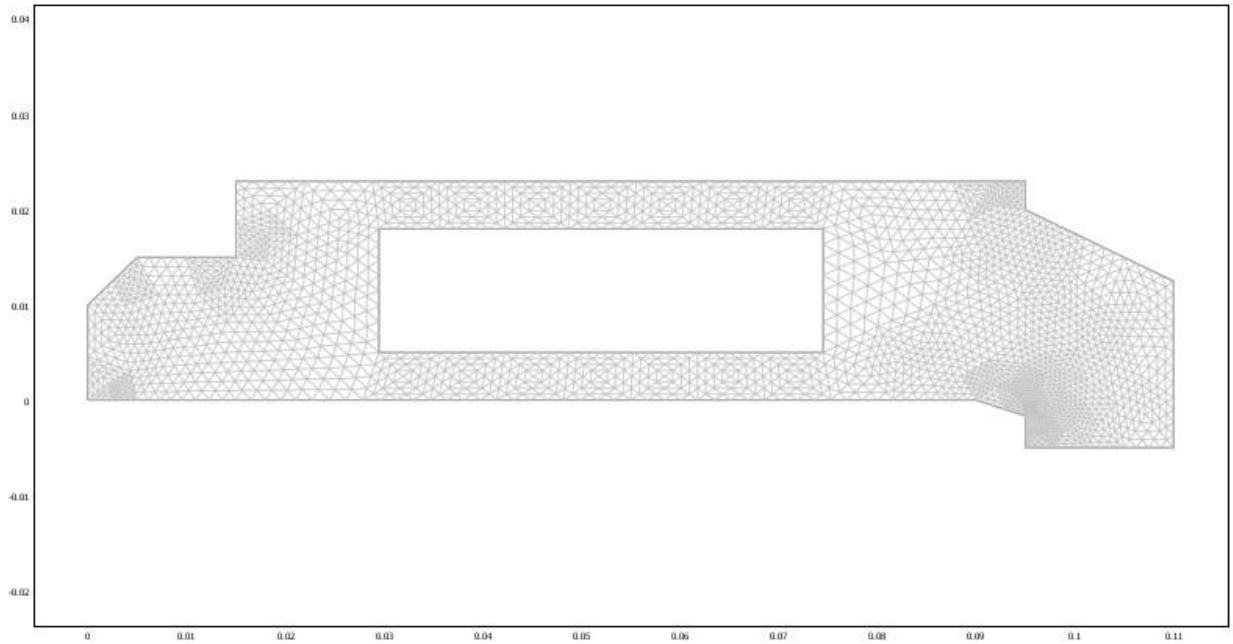

Figure 3. Unstructured mesh of nasal cavity, containing 4624 triangular elements. Predefined mesh size was extra fine.

3.4 Governing Equations

The lower region of the nasal passage way was determined by literature research with accurate dimensions (Inthavong *et al.,* 2008). To model the intake of air via the nose, the Navier Stokes equation was used to describe air as an incompressible fluid. The 2D Navier-Stokes and steady state continuity equations in Cartesian coordinates are shown in Appendix A (Datta and Rakesh 2008).

To account for the drug particles within the nasal spray, the velocity of the particles were determined with the Lagrangian equations shown in Appendix A (Inthavong *et al.* 2008).

3.5 Boundary Conditions

The boundary conditions used in our model are shown in Figure 4, below. This is a representation of our boundary conditions. At the nostril inlet, we have a constant airflow velocity. At the outlet going into the pharynx, we have a neutral condition, which translates to zero pressure in this case. All other boundaries have a no slip condition and 100% particle

trapping. We have divided the nasal cavity into the anterior, turbinate, and posterior portions. Spray is most often deposited in the anterior of the nasal cavity, but ideally deposition is desired in the vascularized mucosal lining of the turbinates.

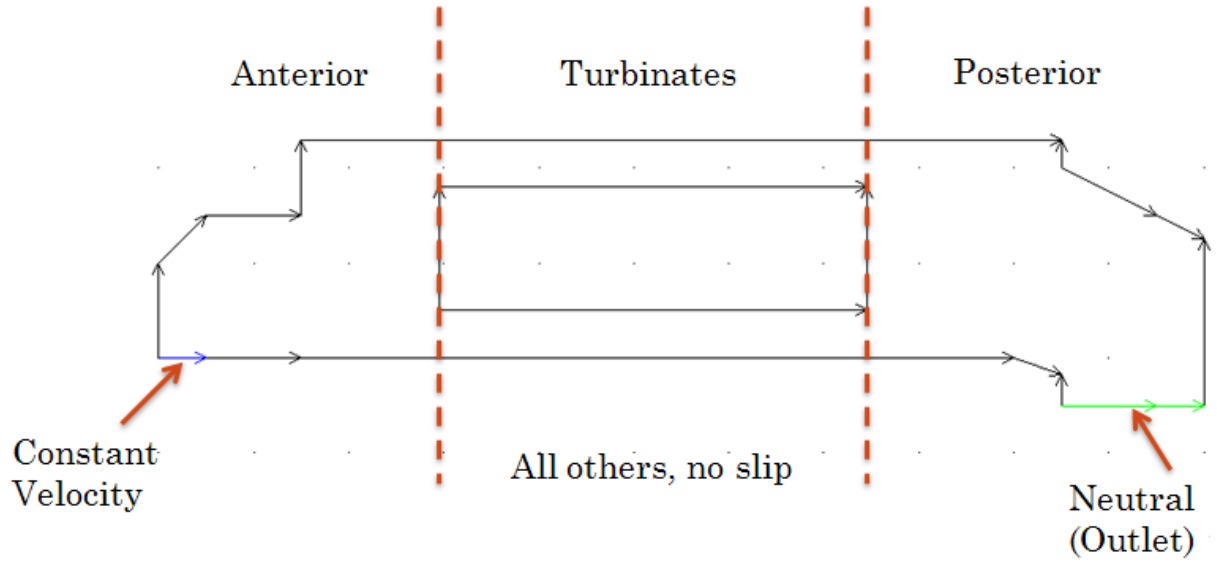

Figure 4. COMSOL geometry boundaries. Left inlet has constant velocity boundary conditions in equal x and y components, resulting in a 45° angle. The nasal spray is inserted at the same angle, and also has a constant spray velocity. At the right (outlet), we have a neutral boundary condition to account for drug particles leaving he nasal passageway to the pharynx. All other boundaries are set to no slip for air flow, and 100% particle trapping for nasal spray particles.

3.6 Assumptions

(Inthavong *et al.* 2008)

Fluid Flow

1. Inspiratory flow rate of 15 L/min (0.9 m/s)
2. Gravity was negligible in air and particle flow
3. Plug flow imposed at the nostrils
4. No slip condition at the walls
5. Laminar Flow
6. Normal velocity gradient was set to 0 at the outlet
7. Nasal walls were rigid (neglecting mucous movement and nasal hairs)

Particles

8. Uniform size
9. Approximated as spheres
10. Same density as water
11. Trapped with 100% efficiency upon touching the wall

12. Brownian and Saffman lift forces were neglected
13. Spray was inserted into the nose and directed parallel to the nasal passage

3.7 Input Parameters

The input parameters and units that we used are shown in Table 1. Initial velocity is split into its x-component, *u*, and y-component, *v*. The subscript *p* denotes particles, and the subscript *g* denotes the fluid (gas phase). The inlet air velocity at the nostrils during breathing was previously shown to be approximately 0.90 m/s (Inthavong *et al.* 2008). We assumed a 45° angle for the direction of flow for incoming air, and calculated the component vectors to be 0.63 m/s in both the x and y directions. Since the nasal spray particles are very small, we used the same initial velocities for both particles and air.

Table 1. Input parameters and units.

Particle Density	ρ_p	1000	kg/m^3	Inthavong *et al.* 2008
Particle Diameter	d_p	50	μm	Inthavong *et al.* 2008
Initial Particle Velocity	v_p	0.63	m/s	Inthavong *et al.* 2008
	u_p	0.63	m/s	
Initial Fluid Velocity	v_g	0.63	m/s	Inthavong *et al.* 2008
	u_g	0.63	m/s	
Drag Force Coefficient	C_d	0.44		Holland *et al.* 1995
Fluid Viscosity at 290K	μ_g	1.7985×10^{-5}	kg/ms	Datta and Rakesh 2008
Fluid Density at 290K	ρ_g	1.2177	kg/m^3	

Calculated Parameters (Inthavong *et al.* 2008)

Reynolds Number	Re_p	7839	
Drag Force per unit particle mass and per unit velocity difference between particle and fluid	F_d	4.65248×10^5	1/s*
Mass of Particle	m_p	5.236×10^{-13}	kg

*Units explained in Appendix A – Particle Velocity

4. Results and Discussion

4.1 Results

We used COMSOL to simulate nasal spray deposition in a simplified 2D geometry at the following baseline conditions: a particle size of 50 μm, particle density of 1000 kg/m^3, inlet particle angle of 45˚, and penetration depth of 0 cm. We simulated 2 seconds of inhalation with a 0.1 second time step in COMSOL. Figure 9 is a plot of fluid velocity with respect to time at the point (0.03, 0.02) in our model. We chose this point because it was at the anterior-turbinate interface, potentially a region of high variability. In the plot, the fluid velocity reaches steady state well before the 2-second simulation time, at approximately 0.5 seconds. Figure 10 shows the results of a surface plot and particle tracing 2 seconds after the start of the simulation. The black lines show the trajectories of the particles and the pink circles show the final deposition location. In this baseline condition, it can be seen that most particle deposition occurred in the anterior region.

Figures 11 and 12 show magnified images of the anterior and posterior-outlet regions, respectively, showing that particles had become trapped in eddy currents. At the outlet, a few particles still follow the eddy current while others are carried to the pharynx. Although many Computational Fluid Dynamics models have employed a no slip condition at the interior boundaries, this may not be a valid assumption. The no slip condition requires that velocity at the walls be set to zero, resulting in particle trajectories that never touch the wall in certain areas. Furthermore, this tendency for particles to not touch the wall – and subsequently be trapped – within the cavity results in more particles being carried to the outlet.

We also examined the effects of penetration depth of the spray nozzle into the nasal cavity. Figure 13 shows a surface plot of these results. We observed that with an increased penetration depth, more particles were carried to the outlet and fewer particles followed eddy currents, when compared to the baseline condition.

4.2 Limitations of Results

During the modeling process, we determined that the particle tracing function had limitations whereby certain parameters resulted in COMSOL fatal memory errors. These errors arose when obtaining a solution with a large mesh size at a variety of particle sizes. The errors were reduced

when using a smaller mesh size of fewer elements but still resulted in errors when the particle size was below 50 μm. In order to obtain results, the resolution size in the particle tracing module had to be decreased to 1, as computation was not possible with higher resolutions. Due to memory limitations of COMSOL, we were not able to run the model with a refined mesh and small particle sizes of 50μm and below as suggested by literature research. The input parameters for the working model are however still within range of the literature research.

4.3 Model Validation

In order to perform an accuracy check on our nasal passage model, we compared our results to a study conducted by Cheng *et al.* (2001) that quantified particle deposition in the nasal cavity. These researchers were able to do so by making an acrylic replica of a human nasal cavity and testing four commercially available nasal sprays with varying cone angles in their model. Cheng *et al.* (2001) elected to test sprays with various cone angles to examine its effect on particle deposition. The deposition varies greatly because of the cone angle difference, since if a spray disperses faster, more deposition would occur early in the anterior region. Spray deposition percentage into the 3 main regions of the nasal cavity: anterior, turbinate and posterior region was quantified by radiolabeling the nasal spray. Results from the Cheng *et al.* (2001) study (Figure 5) illustrate that most of the spray deposition occurs in the anterior and turbinate regions.

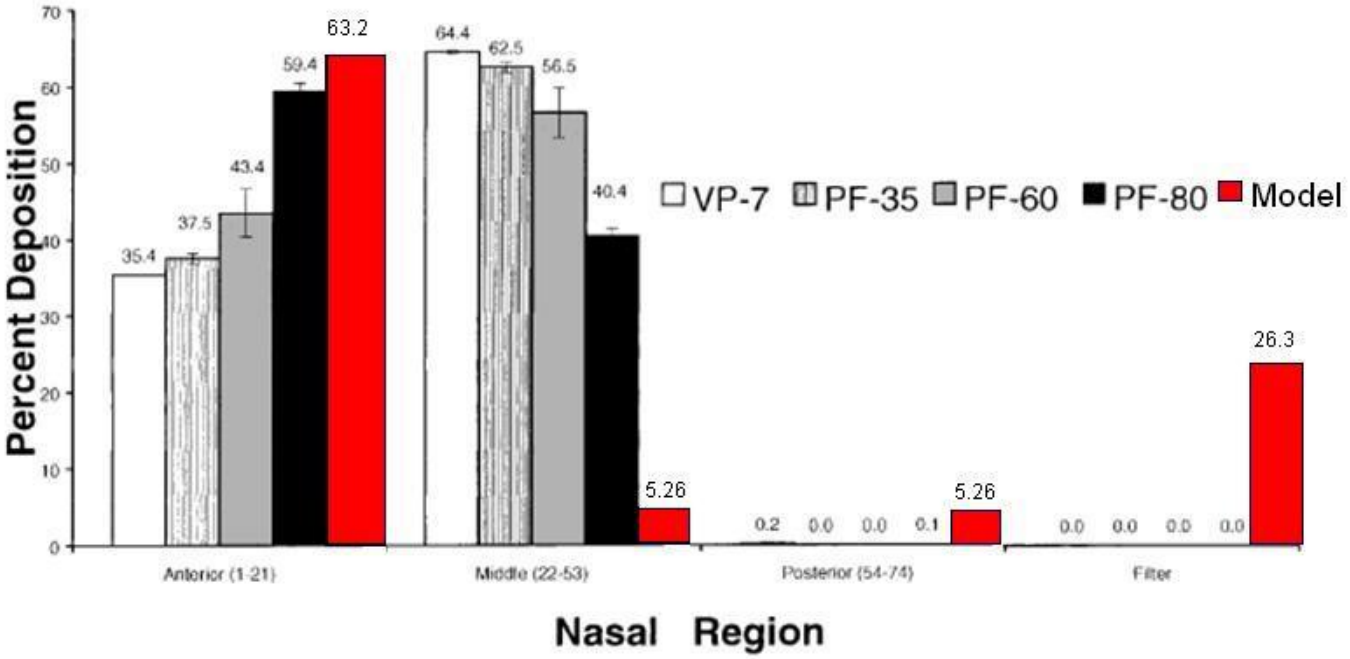

Figure 5. Four commercial sprays (VP-7, PF-35, PF-60, and PF-80) of various cone angles were tested to demonstrate nasal spray deposition patterns (Cheng *et al.* 2001). Results from our model were superimposed onto their data.

Using the particle tracking function in COMSOL, we were able to visualize the locations of the deposition and perform the same analysis to compare our model with results from this paper. Our model tracked 19 particles from the nostril inlet. We found that 63.2% of the particles were deposited into the anterior portion, 5.26% in the turbinates, 5.26% in the posterior portion and 26.3% exited through the outlet (Figure 5). We see that our results for the anterior portion essentially mimic the results from the PF-80 (Cone Angle: 70°) nasal spray types used in the Cheng *et al*. (2001) study at 59.4%; however, we found a significant difference in percentage of the particles carried to the outlet. This can be attributed to the fact that the air flow velocities in the two studies varied (Q, or flow rate, varied by 5 L/min). Furthermore, differences between the experimental study and our model are likely due to the fact that there is an upper turbinate in the experimental setup, which has a more accurate 3D geometry from MRI scans. The difference in deposition in the turbinate region is likely because the experimental 3D geometry had more surface area in this region for the particles to deposit.

4.4 Sensitivity Analysis

For our sensitivity analysis, we examined the effects of the following parameters: spray angle, penetration depth, particle size, and density of the nasal spray. Our initial values for the study for

density, spray angle, particle size and penetration depth were 1000 kg/m^3, 45°, 50 µm diameter and 0 cm (level of nostril inlet), respectively. Spray angle, particle size, and density of the nasal spray fluid were varied in a range of the baseline value ±40%. We also tested 3 different penetration depths: 0, 0.5cm, and 1.0 cm into the nostril. We were able to perform the sensitivity analyses by tracing the particles to specific regions defined in the nasal geometry: the anterior (front) portion before the turbinates, the middle turbinate region, the posterior region following the turbinates, and the nasal passage outlet (Figure 4). We counted the particles in each of the regions and displayed the data (Figure 6) as a percentage of the total particles in the system.

We found that the resulting particle deposition pattern was insensitive to all of the tested parameters except for penetration depth. Increasing penetration depth into the nostril results in an increased percentage of particles that exit through the outlet, while decreasing deposition in the anterior region of the nasal cavities; however, deposition in the middle and posterior regions were relatively insensitive to variation in penetration depth. The changes due to penetration depth are expected because by decreasing the distance between the deposition area and the nozzle inlet, it is easier for the particles to begin flowing with the inhaled air than if the particles were sprayed directly at the level of the nostril inlet.

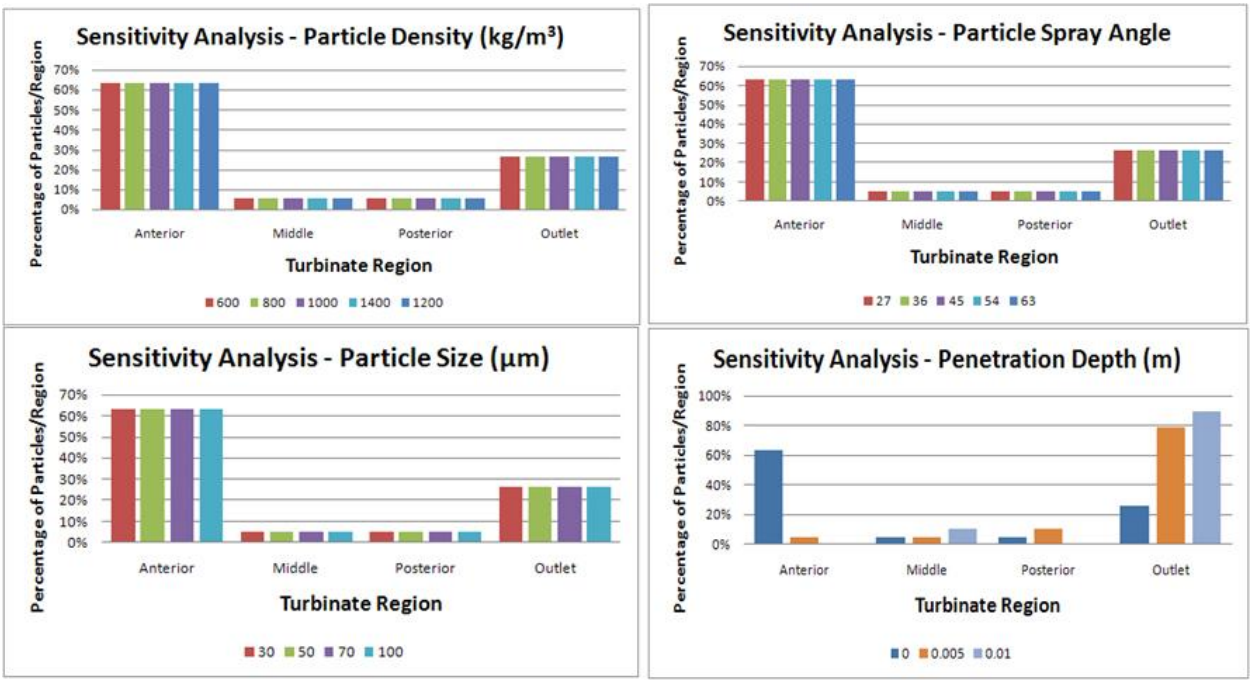

Figure 6. Results for sensitivity analysis. The parameters that we varied were particle density, spray angle, particle size and penetration depth. We varied the particle density, spray angle and particle size in 20% and 40% increments from the initial. We varied penetration depth from the bottom of the nostril in 5mm and 1cm increments. Sensitivity analyses were done by observing the percentage of particles depositing in the following regions in the nasal cavity: anterior (front), middle (turbinate), posterior (back) and through the passage outlet.

5. Conclusions and Design Recommendations

Nasal sprays are an alternative method for drug delivery compared to oral and IV administration. This method has been applied to cold and allergy symptoms, flu vaccinations (Jackson *et al.* 1999), smoking cessation (Hjalmarson *et al.*, 1994), and migraine headaches (Graff and Pollack, 2005). Recent work has been done for those who suffer from diseases where daily administration of drugs is necessary, such as diabetes patients. Recently, nasal sprays have been researched for delivery of insulin via enhancer molecules (Dondeti *et al.*, 1995).

These treatments have been effective as nasal drug delivery provides a faster response to the blood stream and avoids the GI tract where drugs can degrade. This avoidance also lessens the nauseous feelings and vomiting that occurs with oral drugs. Additionally, because of the ease of use, there is high patient compliance with nasal sprays as they are less painful and provide fast relief (Inthavong *et al*. 2008).

5.1 Implications and Relevance

Our sensitivity analysis reveals that particle motion in the nasal passage does not vary with changes in particle size and density, leading us to conclude that intranasal drug delivery can be applied to many different kinds of drug particles with varying sizes and densities. Due to this finding, there is a great potential to package many different types of drugs for rapid delivery to the bloodstream or area of interest. Implications to this design can be applied to immune system recognition, encapsulation techniques and nanofabrication.

Drugs targeted to the immune system, such as vaccinations, require time for the immune system to actively recognize the antigen presented to the bloodstream. Therefore, spray powder formulations have been proposed to allow for more time-dependent vaccine delivery in the mucosa. This can be accomplished by coating the antigen or drug molecule in materials such as starch and poly(acrylic acid) (Coucke *et al.* 2009). It has also been shown that chitosan, a material derived from a naturally occurring polysaccharide with low cytotoxicity, can also serve as an encapsulation material. Chitosan is a unique biological material as it has the ability to

temporarily open tight junctions in the epithelial cell layer to allow for better delivery into the blood vasculature. Additionally, nanofabrication techniques have been applied in to nasal spray delivery with respect to the self-assembly of liposome drug encapsulations. This would account for more lipid-soluble drugs in the nasal mucosa (Sharma *et al*. 2009).

In each of these systems, the encapsulation process increases the size of the particulates. However, our study observed that deposition is insensitive to particle size and density, so larger drugs will have the same particle deposition patterns as smaller drugs. Larger drugs have further advantages as the particle load can be protected from first line defense mechanisms of the immune system. The particle size does have to be within a range as it will otherwise not diffuse through the mucosal layers for effective relief.

5.2 Design Recommendations

We were able to determine that our model was insensitive to particle size, particle density and spray angle. This allows for flexibility in drug design. For example, drugs can be loaded into protective coatings that increase the load size without affecting the particles' flow in the nasal passage. This finding shows that nasal sprays can be utilized to deliver larger particles with a consistent deposition pattern, including polymer or chitosan encapsulations. Because particle density does not play such a role in the intranasal model, several drug formulations can be used, allowing patients to choose a less invasive drug delivery method if shots are not an option due to fear or even in an extreme case, hemophilia. An insensitivity to spray angle is significant because at the user level, a patient administering the drug would not need extensive training to use a nasal spray device. The spray nozzle would have to be inserted into the nostril and drug could be delivered without mention of not delivering enough or too much drug per dose. This finding provides a user-friendly interface that is more universal since all people may either spray differently or have slightly different nasal geometry.

Another important consideration for design of intranasal sprays lies in the user interface because our model was very sensitive to penetration depth. Since penetration depth can affect the model so greatly, a nasal spray should be designed with a stopper outside of the nozzle to indicate the optimum penetration depth. A nasal spray would need such control of this variable in order to be an effective drug delivery method. Because penetration depth affects the model greatly, it could be possible to administer the drug to certain tissues using our simulation methods. In order to

target the central nervous system, the olfactory bulb in the nasal cavity would provide a more direct way to bypass the blood-brain barrier (Graff *et al*. 2005). A simulation in this case could return an optimal penetration depth at which drug deposition occurs mostly at the olfactory bulb region. Also, it was stated that the most favorable target in the respiratory tract for drug delivery to systemic circulation was in the alveolar region, especially due to a large absorptive surface (Laube 2005). As we increased penetration depth, more particles were exiting through the outlet and thereby depositing past the nasal mucosa and into the lower respiratory tract. Due to this, we propose that a CFD simulation could also help target the systemic circulation.

5.3 Design Constraints

In modeling the nasal passageway to observe drug deposition, we were limited by COMSOL memory usage and simplified geometry. We were able to implement the Navier Stokes equation to account for air flow but had trouble with accurate particle quantification. In many trials when using the *Particle Tracing* function, we encountered fatal errors due to maximum memory usage. This occurred even with low resolution and few numbers of particles.

We also simplified our model and compressed the geometry to only account for one nostril in 2D with only a lower turbinate, neglecting the upper turbinate fold. As the turbinate folds were evaluated as perfect rectangular obstructions in the nasal passageway, the fluid flow resulted in eddy currents. Furthermore, as our model for nasal deposition and geometry was approximated based on nasal images of a single person's nasal cavity, we are not modeling a universal population. However, our studies give us a general picture of nasal air flow and particle deposition, since particle deposition was insensitive to changes in many variables. Overall, COMSOL proved to be an invaluable tool to model a complex particle flow in the nasal cavity without time-intensive in vitro or in vivo experimentation using real spray formulations.

Many of the design recommendations of this study are pertinent to design of user-friendly packaging for nasal sprays, which can be implemented without significant cost to the manufacturer. We also showed that various drug formulations can be used, encompassing a large range of particle sizes and densities. Economical constraints of specific formulations should be considered.

6. Appendix A: Mathematical Statement of the Problem

Governing Equations

(Inthavong *et al.* 2008)

Air Flow – Continuity and Navier Stokes

$$\frac{\partial}{\partial x}\left(\rho_g v_g\right) = 0$$

$$\rho\frac{\partial v_x}{\partial t} + \rho\left(v_x\frac{\partial v_x}{\partial x} + v_x\frac{\partial v_x}{\partial y}\right) = -\frac{\partial p}{\partial x} + \mu\left(\frac{\partial^2 v_x}{\partial x^2} + \frac{\partial^2 v_x}{\partial y^2}\right) + \rho g_x$$

$$\rho\frac{\partial v_y}{\partial t} + \rho\left(v_y\frac{\partial v_y}{\partial x} + v_y\frac{\partial v_y}{\partial y}\right) = -\frac{\partial p}{\partial y} + \mu\left(\frac{\partial^2 v_y}{\partial x^2} + \frac{\partial^2 v_y}{\partial y^2}\right) + \rho g_y$$

Particle Velocity – Lagrangian Particle Tracing

$$m_p\frac{dv_p}{dt} = \left[F_d\left(v_g - v_p\right)\right]m_p$$

$$F_d = \frac{18\mu_g}{\rho_p d_p^2}\frac{C_d Re_p}{24}$$

$$Re_p \equiv \rho_p d_p\frac{\left|v_p - v_g\right|}{\mu_g}$$

Drag force per unit particle mass is described by the expression: $F_d\left(v_g - v_p\right)$

where the units of F_d are in inverse time.

7. Appendix B: Solution Strategy

7.1 Detailed COMSOL Implementation

Fluid Flow

The fluid flow was modeled via the transient Navier Stokes equation for an incompressible fluid.

Particle Motion

To model the motion and deposition of nasal spray droplets, we used the Particle Tracing function of COMSOL (Figure 7), which can be found at: "*Postprocessing* > *Plot Parameters* > *Particle Tracing.*"

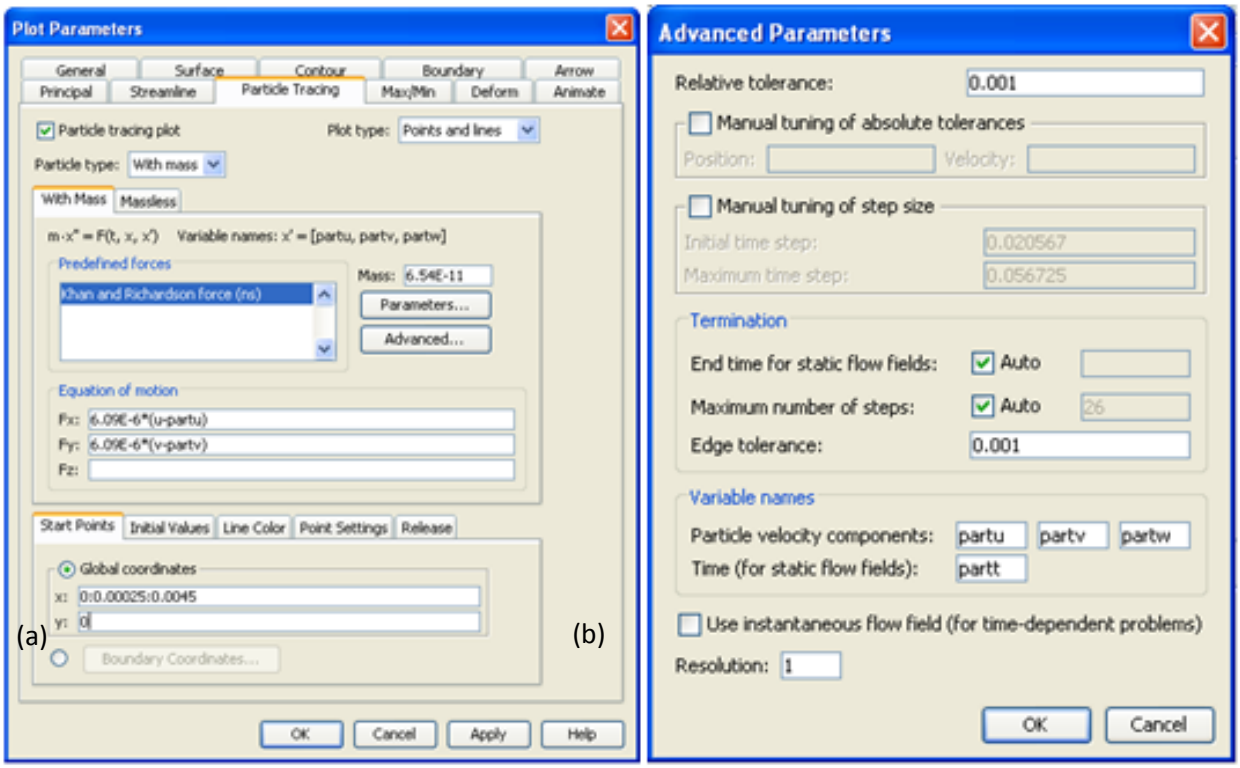

Figure 7. Particle Tracing Menus. (a) Particle Tracing tab in Postprocessing > Plot Parameters. Clicking on the "Advanced..." button brings up the (b) Advanced Parameters window, in which we can decrease the Resolution to decrease computation time.

7.2 Mesh Convergence

Mesh convergence analysis (Figure 8) was performed by calculating the average x-component of air velocity in the nasal cavity model in COMSOL, at time t = 0.2 seconds. We chose an early time because the nasal deposition modeled by COMSOL particle tracing was a transient process, and we found that the particles were deposited within the first second of airflow. Furthermore,

0.2 seconds is the time before the model reaches steady state air flow patterns, and thus contains the most variability. We chose to use the x-component of air velocity because it contains the most variability, as well as for ease of calculation.

Average x-component of air velocity was found by using the Postprocessing Subdomain Integration function of COMSOL (Datta and Rakesh 2008). For each mesh, we performed the following subdomain integration: (1) Expression: U_ns, Subdomain: all; and (2) Expression: 1, Subdomain: all (area integral). The average air velocity was calculated as

$$Average\ Air\ Velocity = \frac{U_{ns}\ integral}{area\ integral}$$

We found that a mesh of 6476 elements was the coarsest mesh to show convergence (Figure 8). Due to memory constraints, however, the mesh with 4624 elements was used in this simulation.

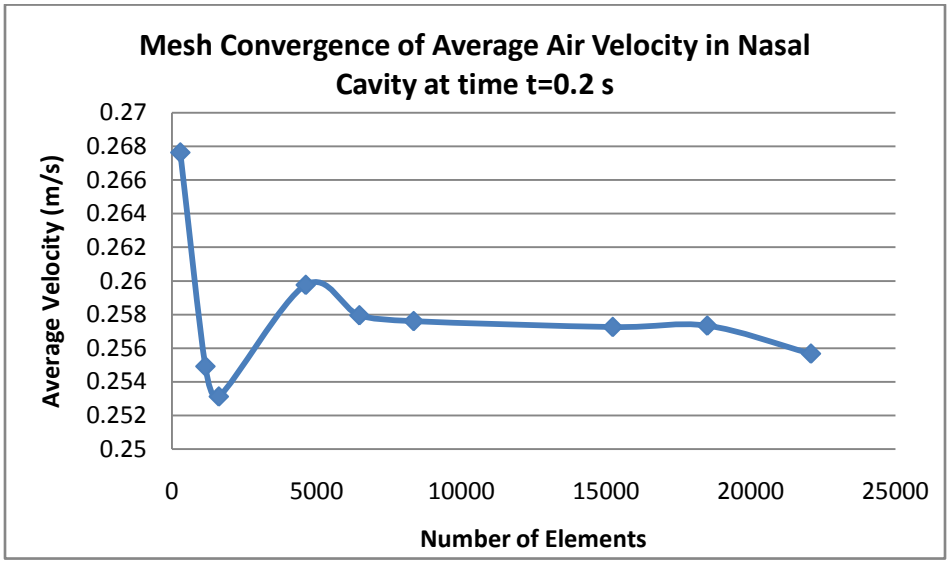

Figure 8. Mesh convergence of average air velocity in the nasal cavity at time t=0.2 seconds.

8. Appendix C: Results

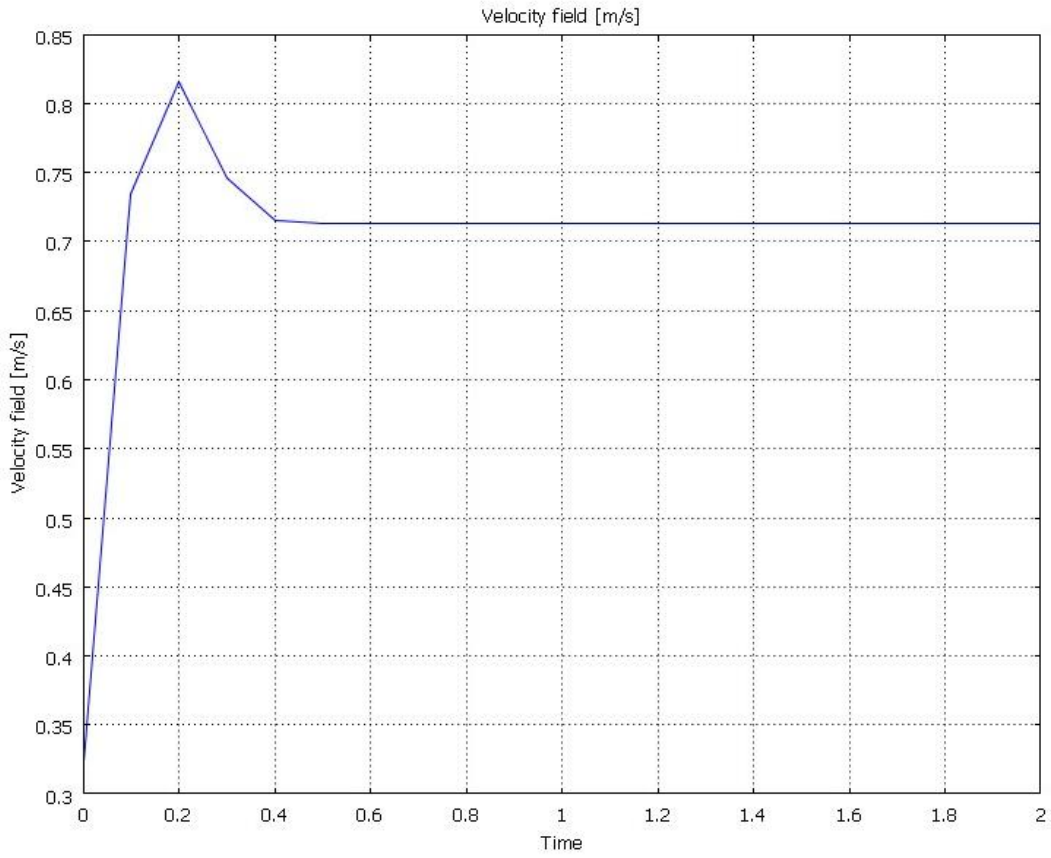

Figure 9. Fluid velocity change with time. This air velocity graph is taken at point (0.03, 0.02) in our model, a point at the interface between the anterior and turbinate regions. At this location, the fluid velocity pattern reaches steady state after only 0.4 seconds of simulation.

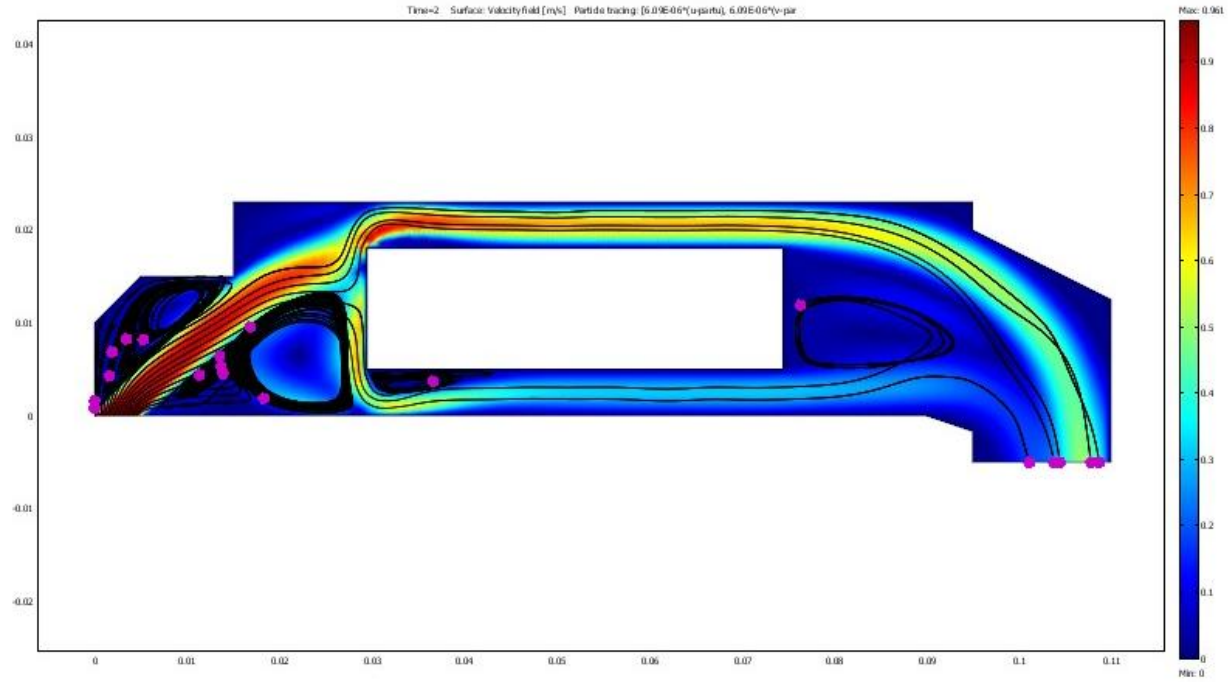

Figure 10. Surface plot with particle tracing after 2 seconds of simulation. The black lines show the trajectories of the particles and the pink circles show the final deposition location. In this baseline condition, most particle deposition occurred in the anterior region.

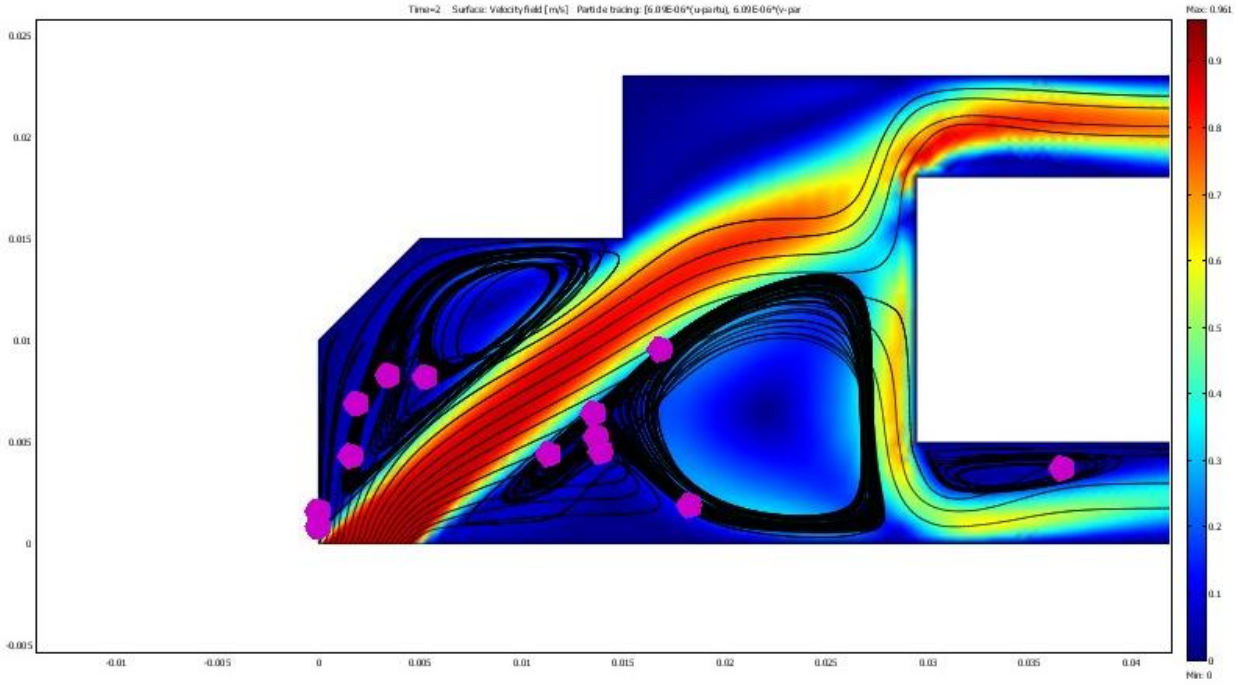

Figure 11. Magnified image of the anterior region at baseline. Due to the air flow and no slip condition at the walls, particles have become trapped in eddy currents caused by the nasal geometry.

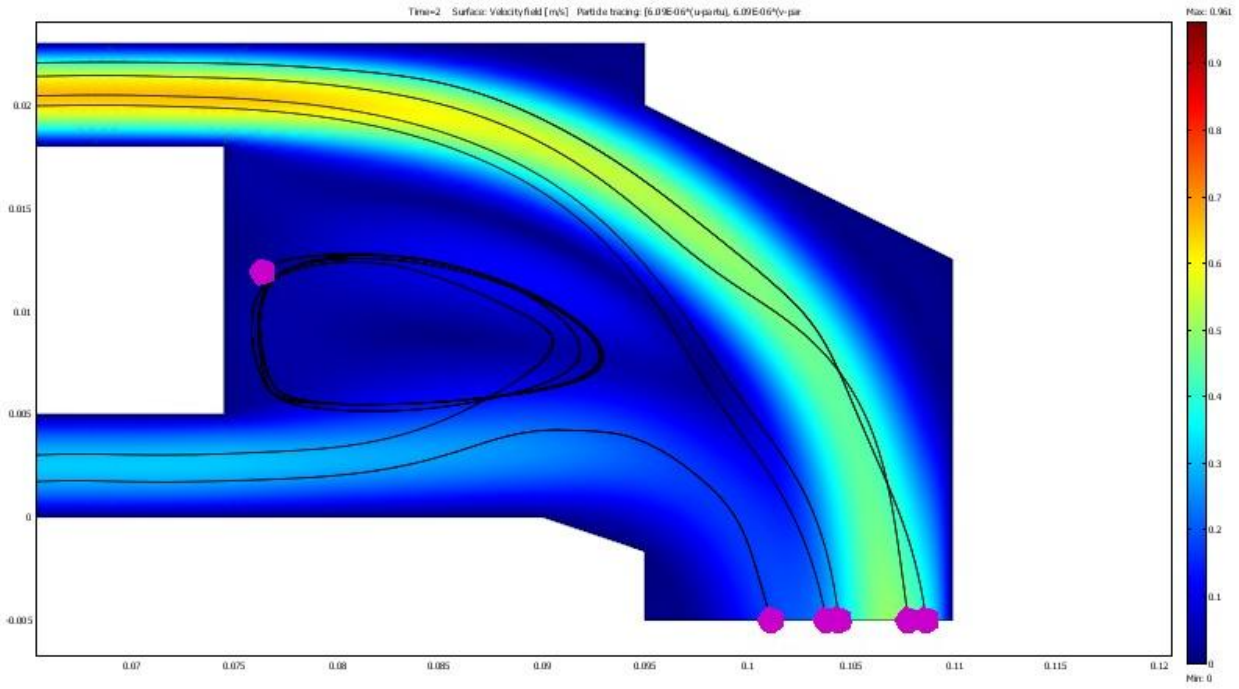

Figure 12. Magnified image of the posterior and outlet regions at baseline. Due to the air flow and no slip condition at the walls, particles have become trapped in eddy currents caused by the nasal geometry. Other particles have been carried through the entire cavity to the outlet, and would proceed to the pharynx.

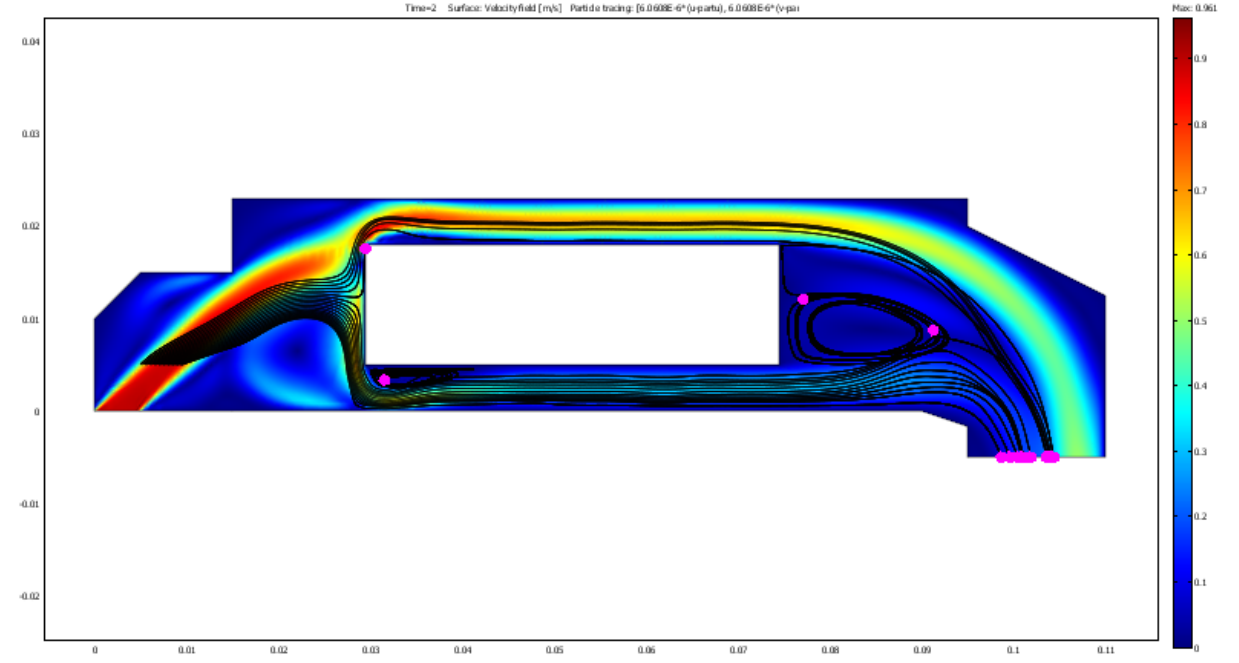

Figure 13. Surface plot with particle tracing at an increased penetration depth. An increase in penetration depth results in an increase in the percentage of particles that are carried to the outlet, and a decrease in deposition in the anterior region.

9. Appendix D: References

1. Born J, Lange T, Kern W, McGregor GP, Bickel U, Fehm HL. 2002. Sniffing neuropeptides: a transnasal approach to the human brain. *Nature Neuroscience.* 5: 514-516.

2. Cheng YS, Holmes TD, Gao J, Guilmette RA, Li S, Surakitbanharn Y, Rowlings C. 2001. Characterization of Nasal Spray Pumps and Deposition Pattern in a Replica of the Human Nasal Airway. *Journal of Aerosol Medicine* 14(2): 267-280.

3. Coucke D, Schotsaert M, Libert C, Pringels E, Vervaet C, Foreman P, Saelens X, Remon JP. 2009. Spray-dried powders of starch and crosslinked poly(acrylic acid) as carriers for nasal delivery of inactivated influenza vaccine. *Vaccine* 27(8): 1279-1286.

4. Datta AK and V Rakesh. 2008. An Introduction to Modeling of Transport Processes: Applications to Biomedical Systems. *Pre-publishing copy. Cornell University Store, Ithaca, NY.*

5. Dondeti P, Zia H, Needham TE. 1995. In vivo evaluation of spray formulations of human insulin for nasal delivery. *Int J Pharm.* 122(1-2): 91-105.

6. Graff CL and GM Pollack. 2005. Nasal Drug Administration: Potential for Targeted Central Nervous System Delivery. J Pharm Sci 94(6): 1187-1195.

7. Hjalmarson A, Franzon M, Westin A, Wiklund O. 1994. Effect of nicotine nasal spray on smoking cessation. Arch Intern Med 154: 2567-2572.

8. Holland FA and R Bragg. 1995. Fluid Flow for Chemical Engineers (2nd Edition). Elsevier. Online version available at: http://knovel.com/web/portal/browse/display?_EXT_KNOVEL_DISPLAY_bookid=412&VerticalID=0

9. Inthavong K, Tian ZF, Tu JY, Yang W, Xue C. 2008. Optimising nasal spray parameters for efficient drug delivery using computational fluid dynamics. *Computers in Biology and Medicine* 38: 713-726.

10. Jackson LA, Holmes SJ, Mendelman PM, Huggins L, Cho I, Rhorer J. 1999. Safety of a trivalent live attenuated intranasal influenza vaccine, FluMist(TM), administered in addition to parenteral trivalent inactivated influenza vaccine to seniors with chronic medical conditions. Vaccine 17(15-16): 1905-1909.

11. Kimbell JS, Segal RA, Asgharian B, Wong BA, Schroeter JD, Southall JP, Dickens CJ, Brace G, Miller FJ. 2007. Characterization of Deposition from Nasal Spray Devices Using a Computational Fluid Dynamics Model of the Human Nasal Passages. *Journal of Aerosol Medicine* 20(1): 59-74.

12. Laube BL. 2005. The Expanding Role of Aerosols in Systemic Drug Delivery, Gene Therapy, and Vaccination. *Respiratory Care.* 50(9): 1161-1176.

13. Nienkamp M, Johnson D, Higginbotham L, "Nasal Anatomy" A.D.A.M. Medical Encyclopedia 2007. Date of Access 4/17/2009 http://adam.about.com/encyclopedia/Nasal-anatomy.htm

14. Pringels E, Callens C, Vervaet C, Dumont F, Slegers G, Foreman P, Remon JP. 2006. Influence of deposition and spray pattern of nasal powders on insulin bioavailability. *Int J Pharm*. 310(1-2): 1-7.

15. Sharma S, Mukkur TKS, Benson HAE, Chen Y. 2009. Pharmaceutical Aspects of Intranasal Delivery of Vaccines Using Particulate Systems. *Journal of Pharmaceutical Sciences* 98(3): 812-843.

16. "Nasal Cavity." Wikipedia: The Free Encyclopedia. 15 April 2009 <http://en.wikipedia.org/wiki/File:Illu_nose_nasal_cavities.jpg > accessed 30 April 2009